



## Rice panicle length measuring system based on dual-camera imaging



Chenglong Huang<sup>a</sup>, Wanneng Yang<sup>a,b,c</sup>, Lingfeng Duan<sup>a</sup>, Ni Jiang<sup>a</sup>, Guoxing Chen<sup>d</sup>, Lizhong Xiong<sup>b</sup>, Qian Liu<sup>a,\*</sup>

<sup>a</sup> Britton Chance Center for Biomedical Photonics, Wuhan National Laboratory for Optoelectronics, Huazhong University of Science and Technology, 1037 Luoyu Rd., Wuhan 430074, PR China

<sup>b</sup> National Key Laboratory of Crop Genetic Improvement and National Center of Plant Gene Research (Wuhan), Huazhong Agricultural University, Wuhan 430070, PR China

<sup>c</sup> College of Engineering, Huazhong Agricultural University, Wuhan 430070, PR China

<sup>d</sup> College of Plant Science and Technology, Huazhong Agricultural University, Wuhan 430070, PR China

### ARTICLE INFO

#### Article history:

Received 16 December 2012

Received in revised form 15 July 2013

Accepted 8 August 2013

#### Keywords:

Rice panicle length

Dual-camera imaging unit

Image processing

Neck identification

### ABSTRACT

The length of the rice panicle determines the number of grains it can hold, and consequently rice yield; it is therefore one of the most important traits assessed in yield-related research. However, the conventional method of measuring panicle length is still a manual process that is inconsistent, subjective and slow. In this study, a novel prototype, dubbed “*Smart-PL*”, was developed for the automatic measurement of rice panicle length based on dual-camera imaging. Cameras with a long-focus lens and a short-focus lens were utilized to capture both a detailed image and a complete image of the rice panicle, respectively. Specific image processing algorithms were exploited, to analyze the neck image for neck identification and the whole-panicle image for path extraction. Subsequently, co-registration was used to identify the neck location in the whole-panicle image, and a resampling method was used to search for the path points between the panicle neck and the tip. Finally, the panicle length was calculated as the sum of the distances between each adjacent path point. To evaluate the accuracy of this prototype, six batches of rice panicles were tested. The results showed that the mean absolute percentage error (MAPE) for the system was about 1.23%, and the automatic measurements had a good agreement with manual measurements, regardless of panicle type. To evaluate the efficiency of this prototype, 3108 panicle samples were tested under continuous-measurement conditions, and the measuring efficiency was approximately 900 panicles per hour, 6 times over manual method. In conclusion, the system automatically extracts panicle length while providing three advantages over the manual method: objectiveness, high efficiency and high consistency.

© 2013 Elsevier B.V. All rights reserved.

### 1. Introduction

Rice is the staple food for approximately half of the world's population (Zhu et al., 2011; Joen et al., 2011). The yield of rice is therefore vital to human survival. From an agronomic perspective, the length of the rice panicle is a major determinant of the number of grains per panicle (Cheng et al., 2007; Kobayasi et al., 2002), which in turn directly determines rice yield (Xing and Zhang, 2010). Consequently, panicle length is a key trait in rice research, such as drought stress research and genetic factor identification, on controlling its traits (Liu et al., 2010; Kato et al., 2009).

Rice panicle length, defined as the length from the panicle neck to the apex (Xiao et al., 1998), is generally measured at the maturity stage. The panicle neck, which has a cyclic structure, is treated

as the dividing point between the stem and the panicle. The manual method of measuring panicle length includes 3 steps: identifying the neck of the rice panicle, straightening the panicle, and measuring the panicle length. Hundreds of new cultivars, produced daily by modern rice breeding methods, need to be evaluated using panicle phenotyping (Bagge and Lubberstedt, 2008). However, the conventional method of measuring panicle length is still manual, which is time-consuming and subjective. Therefore, it is imperative to develop an efficient technology to measure panicle length for rice plant evaluation.

Agriphotonics has been widely used in plant phenotyping research, such as in high-throughput measurements for rice tillers (Yang et al., 2011) and in rapid discrimination and counting of filled/unfilled rice spikelets (Duan et al., 2011). However, little work has been reported on the development of automatic panicle length measurement technology. Scanalyzer 3D Plant Phenotyping, a system developed by LemnaTec Corporation, can estimate rice

\* Corresponding author. Tel.: +86 27 8779 2033; fax: +86 27 8779 2034.

E-mail address: [qianliu@mail.hust.edu.cn](mailto:qianliu@mail.hust.edu.cn) (Q. Liu).

panicle length in vivo ([http://www.lemnatec.com/sites/default/files/application-sheets/2009/12/24/18\\_LemnaTec\\_RiceScanalyzer\\_3D.pdf](http://www.lemnatec.com/sites/default/files/application-sheets/2009/12/24/18_LemnaTec_RiceScanalyzer_3D.pdf)).

([http://www.lemnatec.com/sites/default/files/application-sheets/2009/12/24/18\\_LemnaTec\\_RiceScanalyzer\\_3D.pdf](http://www.lemnatec.com/sites/default/files/application-sheets/2009/12/24/18_LemnaTec_RiceScanalyzer_3D.pdf)), however few details are made public and panicle neck cannot be recognized in the system. Software developed by Ikeda et al. (2010) was able to extract panicle length from scanned photographic images of spread-out panicles (Ikeda et al., 2010). To acquire the images, the panicles were glued in a single layer on a clear sheet and then scanned with a transmission scanner. However, with the complicated preprocessing and low-efficient imaging mode, panicle image acquisition was time-consuming and thus was not suitable for high-throughput measurements. Therefore, development of a system for the automatic measurement of panicle length, with high throughput and high precision, would be valuable for rice breeding.

To accurately measure rice panicle length, it is critical to identify the panicle neck, which is difficult because of the minor differences between the neck and the stem. To identify the neck, high-resolution imaging is needed, but, with most cameras, increasing spatial resolution reduces the field of view (FOV) (Wyant and Schmit, 1998). Theoretically, a camera with a sufficient array size can provide both high spatial resolution and a large FOV. However, large image sizes would lead to long image-processing times. In addition, high-resolution cameras are too expensive for widespread use. Dual-camera imaging, which can be used to acquire two specific images with different valuable information, is a common imaging modality widely used in the detection of poultry carcasses in food (Chao et al., 2002), the row detection of paddy rice seedling in agriculture (Kaizu and Imou, 2008), small animal imaging and medicine (Yang et al., 2010; Jung et al., 2009). This method can provide both high spatial resolution for panicle neck identification and (via a different lens) a large enough FOV to image the whole panicle. Given its measuring efficiency and relatively low hardware cost, dual-camera imaging was preferred for the current work.

The objective of this study is to develop an automatic system called *Smart-PL* for high-throughput, high-precision and low-cost measurement of rice panicle length, and finally provided a practical tool for rice breeding. To achieve it, dual camera imaging method was demonstrated, and the specific image processing algorithms for neck identification, path extraction and panicle length extraction were proposed in the study.

## 2. Materials and method

### 2.1. Materials

The panicle samples used in this paper are shown in Fig. 1. The rice varieties of Huageng 295 and Zhonghua 11 were utilized, which had significant morphological differences. Besides, the fresh harvested rice panicle and sun-dried panicle were both tested, because the span of measurement period is actually long and there is obvious color difference between them. In addition, panicle samples with neck cut off were used to test path extraction, and specialized panicle samples were measured to evaluate neck identification.

### 2.2. System description

#### 2.2.1. Rice panicle length measuring system

The prototype of *Smart-PL* system is shown in Fig. 2b. The system consisted of two conventional white fluorescent tubes, a charge-coupled device (CCD) camera (DH-SV1410FC, Daheng Corporation, China) equipped with a long-focus lens (Computer Corporation, Japan), a CCD camera (DH-SV1410FC, Daheng Corporation, China) equipped with a short-focus lens (Computer Corporation, Japan), a sample presentation platform, a photoelectric switch, a programmable logic controller (PLC, CP1H-Y20DT-D, Omron, Japan), a computer workstation (HPZ600, Hewlett-Packard, USA), and a chamber. Two white fluorescent tubes were employed to provide uniform illumination. The whole-imaging devices were placed in the chamber, and an interface on the chamber was designed for manual operation.

To enhance the contrast of the image and clearly show the spread of the rice panicles, the sample presentation platform (Fig. 2c) was blackened and installed at an angle. In the middle of the platform, there was a groove to hold the panicles in place. The cameras were set on a panel parallel to the sample presentation platform. To ensure that the panicle neck was in the field of view, the camera with the long-focus lens (detailed camera) was placed close to the operation interface. To obtain an image of the entire panicle, the camera with the short-focus lens (whole-field camera) was located above the center of the sample presentation platform. The photoelectric switch in Fig. 2a was connected to the PLC for the detections of putting panicle in and panicle re-

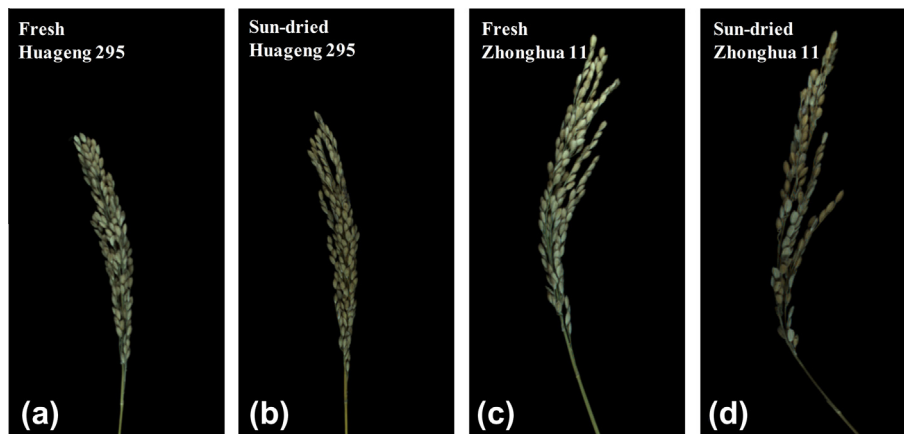


Fig. 1. Rice panicle samples.

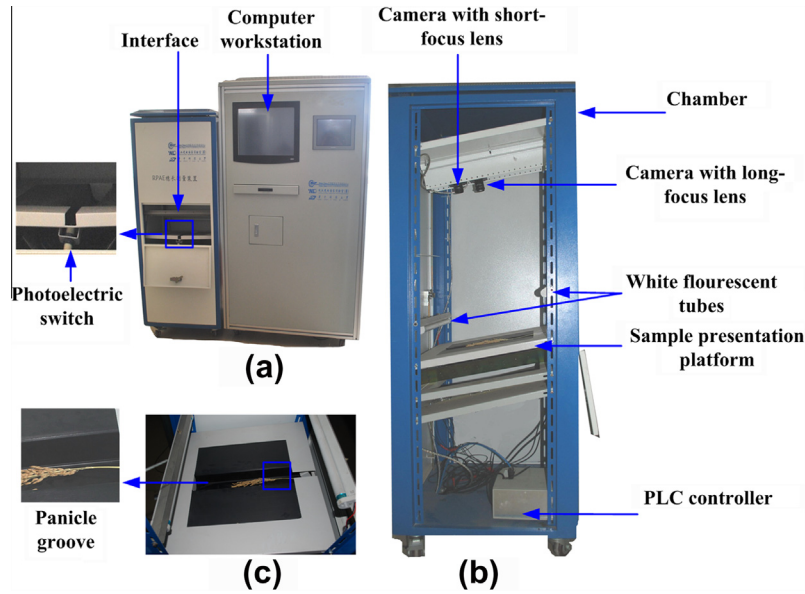


Fig. 2. Smart-PL system: (a) the prototype of the system, (b) the details of the imaging device, and (c) the sample presentation platform.

movement, and the PLC communicated with the workstation to trigger the image acquisition.

2.2.2. Dual-camera imaging unit

The camera in the system has different spatial resolution and FOV with different focus lens and their main features are listed in Table 1. The neck images with different focus lens are shown in Fig. 3. To provide enough spatial resolution for neck imaging, a 35 mm lens was therefore installed in the detailed camera, and a 16 mm lens was mounted in the whole-field camera to offer sufficient FOV (Maximum length 370 mm) for whole panicle imaging.

2.3. System control

The software for the workstation was developed by LabVIEW 8.6 (National Instruments, USA) and Visual Studio (Microsoft, USA). In the software, the automatic observation and resulting image for each panicle were displayed and stored systematically according to a corresponding barcode. In addition, the PLC was programmed by CX-Programmer 7.3 (Omron, Japan).

The system control flowchart included the following steps. (1) The photoelectric switch makes an effective response as a panicle is placed onto the sample presentation platform. (2) At the falling edge of the photoelectric switch's effective response, the PLC informs the imaging system to capture a whole-panicle image and a neck image. (3) After image acquisition, the images are processed with computer vision algorithms in order to determine panicle length. (4) The results, including observations and images, are displayed and stored. (5) When the panicle is removed manually, the

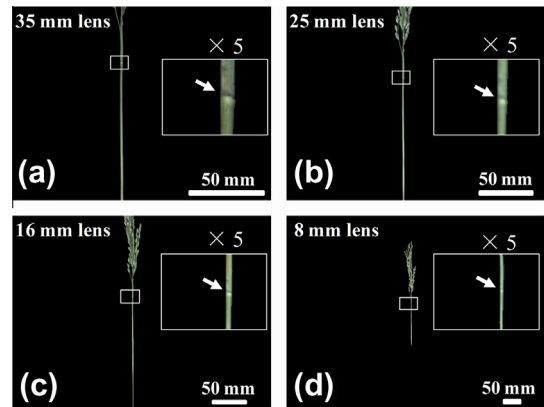


Fig. 3. Neck images with four focus lens: 35 mm, 25 mm, 16 mm, 8 mm; the white rectangles indicated the magnified neck region by 5 times and the white arrowheads pointed necks.

photoelectric switch makes an ineffective response, pending the next panicle measurement. The effectiveness of the photoelectric switch response is controlled and determined by the PLC.

According to the control procedure, the system generally worked with five steps: putting panicle in, image acquisition, image processing, results storage, and taking panicle out. And the time costs for each step were indicated by  $T_i$ ,  $T_a$ ,  $T_p$ ,  $T_r$  and  $T_o$  respectively. Therefore, the time taken to extract the length of each panicle can be represented by the following equation:

$$T = T_i + T_a + T_p + T_r + T_o \tag{1}$$

Table 1  
Main characteristics of the camera with different focus lens.

Characteristic	Camera with 35 mm lens	Camera with 25 mm lens	Camera with 16 mm lens	Camera with 8 mm lens
Sensor	CCD, 2/3 in.			
Array size	1392 × 1040			
Spatial resolution per pixel	0.122 mm × 0.122 mm	0.170 mm × 0.170 mm	0.266 mm × 0.266 mm	0.533 mm × 0.533 mm
Field of view	169 mm × 126 mm	236 mm × 176 mm	370 mm × 277 mm	739 mm × 551 mm
Pixel size	6.45 μm × 6.45 μm			
Maximum frame rate	15 Frames per second			
A/D resolution (bit)	12			
Power consumption	3.0 w and 12 v			

## 2.4. Image process

The whole-field camera captured the whole panicle image (Fig. 4a), and the detailed camera captured the neck image (Fig. 4d). The processing procedure for the whole panicle image mainly involved image segmentation (Fig. 4b) and path extraction (Fig. 4c). Accordingly, the processing procedure for the neck image primarily entailed image segmentation (Fig. 4e) and neck identification (Fig. 4f). Then, co-registration and resampling algorithms were applied for panicle-length extraction (Fig. 4g). And the details of these procedures were presented below.

All the image-processing algorithms were developed in LabVIEW 8.6, except for the algorithms of path extraction and neck identification, which were programmed in the C language and compiled into a dynamic-link library (dll) for LabVIEW calling.

### 2.4.1. Path extraction

The analysis procedure for the whole panicle image is shown in Fig. 5A. Firstly, the region of interest (ROI) in the panicle image was extracted (Fig. 5Aa). During image segmentation, background subtraction and green channel extraction were implemented to acquire a gray image. Then, an automatic threshold calculated by Otsu method (Otsu, 1979), was used to separate the panicle from the background (Fig. 5Ab). To optimize the skeleton extracted in path extraction, operations to fill holes and remove small objects were adopted for image simplification and noise reduction (Fig. 5Ac).

After image segmentation, path extraction was achieved as follows: (1) a subfield-based parallel thinning algorithm (Nemeth and Palagyi, 2011) was used to extract the panicle skeleton (Fig. 5Ad), and (2) a maximum path extraction algorithm to obtain the main path (Fig. 5Ae) was applied, following the steps described in detail. Step 1: Finding all the endpoints (points with only one foreground point in an 8-point neighborhood) and taking the point at the bottom as the starting point. Step 2: Choosing a discretionary endpoint. Step 3: Calculating the connected pixel number from the starting point to the chosen endpoint as the path length. Step 4: Returning to step 2 until all the endpoints are used to obtain all the path lengths. Step 5: Obtaining the maximum path and removing the other branches.

### 2.4.2. Neck identification

The neck image was processed following the procedure depicted in Fig. 5B. In the preprocessing, the neck image (Fig. 5Ba) removed the background as shown in Fig. 5Bb. Then, The ROI extraction and green channel extraction was implemented to obtain a gray image (Fig. 5Bc).

After that, neck identification was achieved as follows. First of all, the stem (Fig. 5Bd) was separated from the spikelets by the

width difference. Secondly, to locate the neck approximately, the stem was divided into several sections (Fig. 5Ca) by stem width ( $Sw$ ), which was calculated by Eq. (2). And the normalized gray change of each section was figured out as the steps: (1) Computing the average gray value of the foreground pixels in each section. (2) Obtaining the average gray change between each adjacent section. (3) Normalizing the gray change by dividing the maximum absolute value. And the final result was shown as Fig. 5Cb. Then, the continuous sections from the minimum difference region to the maximum difference region were regarded as the approximate neck region and marked with red color (Fig. 5Be). At last, the foreground pixels of the marked region were calculated for a threshold value by Otsu method (Otsu, 1979), and the threshold value was adopted to identify the neck with white color (Fig. 5Bf).

$$Sw = \frac{1}{N} \sum_{i=1}^N w_i \quad (2)$$

where  $w_i$  indicates the foreground pixel number in each row of the stem. And  $N$  indicates the line number in the stem.

### 2.4.3. Panicle length extraction

The panicle length extraction was carried out, following the procedure in Fig. 5D. As described above, the neck image (Fig. 5Da) was analyzed to identify the neck (Fig. 5Db) and the mean ordinate of pixels in neck region with white color was calculated as the neck position (in the red line). Meanwhile, the whole panicle image (Fig. 5Dc) was processed to extract the maximum path (Fig. 5Dd). After that, the panicle length was extracted with co-registration, resampling, and panicle length computation. And the details were described below.

Prior to the experiment, the neck image and the whole panicle image were co-registered in two steps. (1) In the FOV of each camera, 8 coins (with a diameter of 25 mm) used as markers, were placed at different positions and the center ordinates of each coin were acquired. (2) Using the two sets of ordinates obtained in the first step, the spatial relationship of the ordinates between the neck image and the whole panicle image was calculated with least squares fitting, as shown by Eq. (3). And the parameters  $a$ ,  $b$  were computed by Eq. (4), which were 0.43 and 742.6 respectively in this system.

$$Y_w = \text{ceil}(aY_d + b) \quad (3)$$

where  $Y_w$  and  $Y_d$  are the corresponding ordinates in the whole panicle image and the neck image, respectively. The function  $\text{ceil}(x)$  returned the value of a number rounded down to the nearest integer.

$$\begin{cases} a = \frac{\sum_{i=1}^n (y_{di} - \bar{y}_d)(y_{wi} - \bar{y}_w)}{\sum_{i=1}^n (y_{di} - \bar{y}_d)^2} \\ b = \bar{y}_w - a\bar{y}_d \end{cases} \quad (4)$$

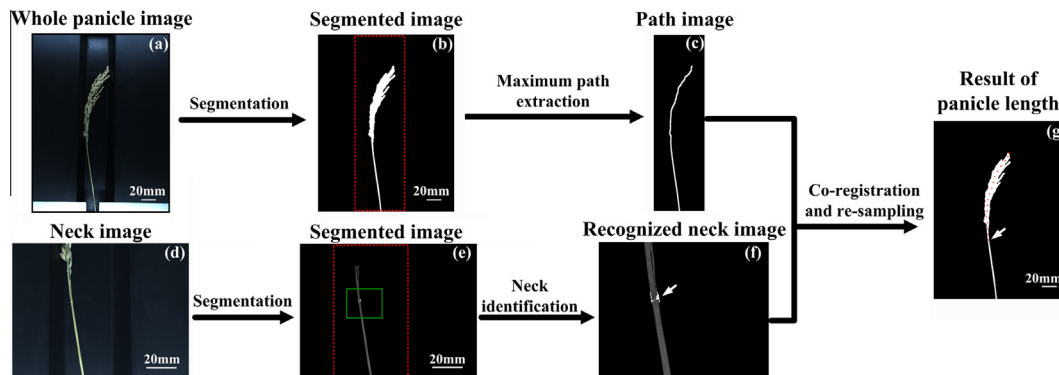
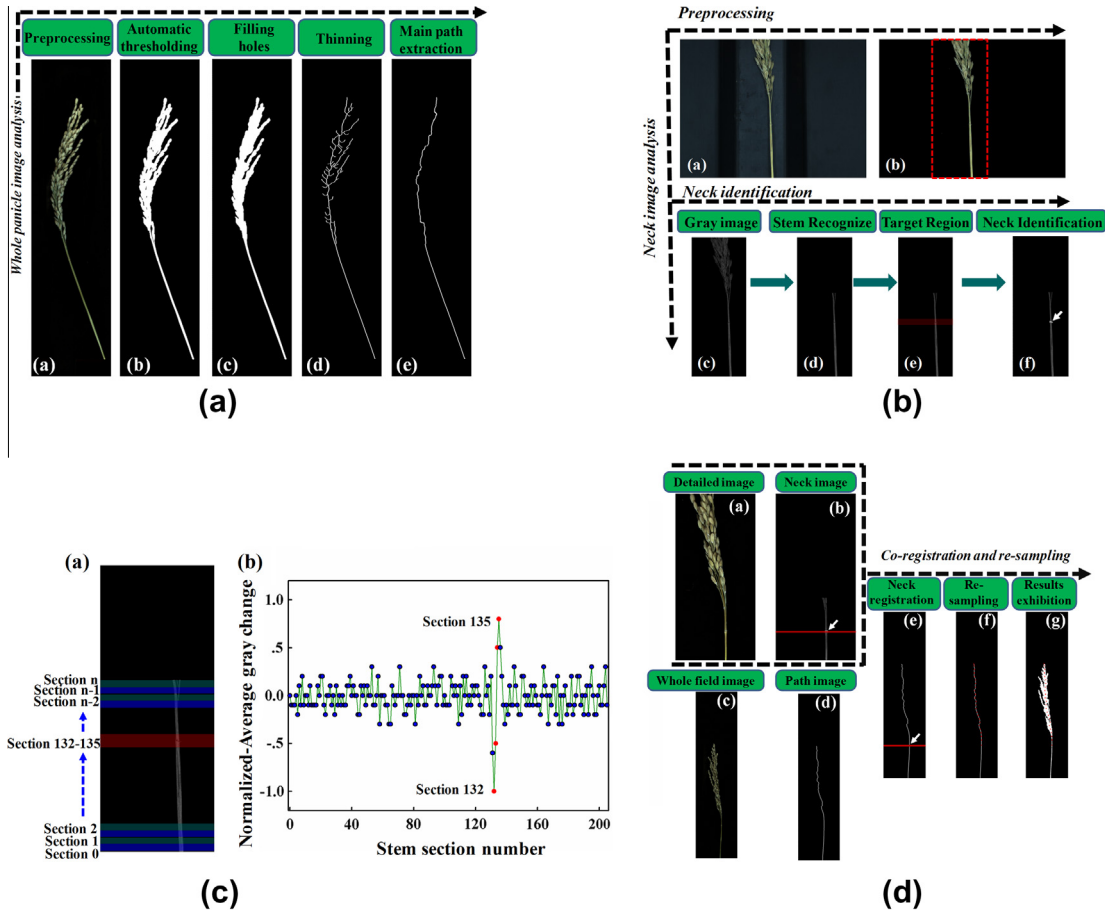


Fig. 4. The image processing procedure in the Smart-PL system; Arrowheads indicated the panicle neck and the red dotted rectangles denoted the region of interest.



**Fig. 5.** Details of the image processing procedure: (A) the whole panicle image processing, (B) the neck image processing; Arrowhead indicated the panicle neck with white color and the red rectangle denoted the region of interest, (C) approximate neck region identification;  $n$  indicated the total section number, and (D) the panicle length extraction; the red line indicated the neck ordinate and the red points represented the panicle length path. (For interpretation of the references to colour in this figure legend, the reader is referred to the web version of this article.)

where  $y_{wi}$  and  $y_{di}$  are the corresponding ordinates of each coin center in the whole panicle image and the neck image, respectively.  $n$  indicates coins number, which are eight in the research. And the parameters  $\bar{y}_w$ ,  $\bar{y}_d$  are the mean ordinates.

Hence, given the neck position in the neck image, the ordinate of the neck in the whole panicle image can be calculated with Eqs. (3) and (4). And the neck position was indicated in the red line (Fig. 5De).

To avoid the zig-zags in the extracted path, resampling was carried out as the following procedures: (1) Dividing the extracted path (from neck to tip) into several pieces at proper sampling interval. (2) Computing the mean coordinate of the points in each piece as the path points. (3) Adding the neck point and tip point into the path points (Fig. 5Df). Consequently, the point set were used to represent the panicle length path. Additionally, the path points were merged with the binary image of whole panicle and the result was exhibited in Fig. 5Dg.

Assuming that the extracted point set was  $(x_i, y_i)$ , the panicle length value denoted by PL was computed by the following equation:

$$PL = R \sum_{i=2}^N \sqrt{(x_i - x_{i-1})^2 + (y_i - y_{i-1})^2} \quad (5)$$

where  $R$  is the spatial resolution per pixel of the camera with the 16 mm lens (0.266 mm/pixel in this system).

### 3. Results and discussion

In general, the measurement errors of the system are caused by the operations for whole panicle image and neck image. To evaluate the whole panicle image analysis accuracy of the system, panicle samples with neck cut off were measured. To evaluate the neck identification accuracy of the system, neck positions in the neck image acquired by system identification and human eyes inspection were compared. Besides, the varieties of Huageng 295 and Zhonghua 11 which had significant morphological differences were tested, to evaluate the adaptability of different varieties. Moreover, the fresh harvested panicles and sun-dried panicles were both measured, since the span of measurement period was actually long and there was obvious difference in color.

Compared with the automatic measurement in the system, manual measurements were performed by three skilled workers, as the following procedure: identifying the neck of the rice panicle, straightening the panicle, and measuring the panicle length. And the mean measuring result was calculated as ground truth. To validate the system measuring accuracy, the root mean squared error (RMSE) defined by Eq. (6) and the mean absolute percentage error (MAPE) defined by Eq. (7) for the panicle length measurement were computed respectively.

In addition, a large number of panicle samples were also tested under the condition of continuous measurement, and the time costs of manual measurement and automatic measurement were compared to test the system's efficiency. Meanwhile, the measur-

ing accuracy was also evaluated to test the reliability and stability of the *Smart-PL* system.

$$RMSE = \sqrt{\frac{1}{n} \sum_{i=1}^n (x_{ai} - x_{mi})^2} \quad (6)$$

$$MAPE = \frac{1}{n} \sum_{i=1}^n \frac{|x_{ai} - x_{mi}|}{x_{mi}} \quad (7)$$

where  $x_{ai}$  represents an automatically measured value by the system and  $x_{mi}$  represents a manually measured value.

### 3.1. Whole panicle image analysis accuracy

To evaluate the whole panicle image analysis accuracy, 100 randomly-selected panicle samples with neck cut off were used to eliminate the measuring error caused by neck identification. And the whole panicle image analysis included following procedures: skeleton acquisition, maximum path extraction, resampling and panicle length calculation. Since resampling was carried out to remove the zig-zags in path extraction and proper resampling interval would be necessary, various resampling intervals were therefore tested in this system.

To evaluate the analysis accuracy of whole panicle image, 100 panicle samples with neck cut off were tested and manual measurement was taken as the ground truth. The distributions of absolute percentage errors (APE) for different resampling intervals are shown in Fig. 6. The results demonstrated that 30 pixels was a proper sampling interval, and this interval value was adopted in the following measurement. If the sampling interval was too small, the MAPE increased significantly because of many zig-zags in the panicle path. On the contrary, if the sampling interval was too big, the MAPE was increased because of the insufficient fitting of the panicle path. And the results of whole image analysis evaluation at the optimal resampling interval are shown in Table 2. From the results, the MAPE and RMSE for the whole image analysis were approximately 0.39% and 1.19 mm respectively. And the squared correlation coefficient ( $R^2$ ) was 0.99. Therefore, it is demonstrated that path points by path extraction and proper resampling as shown in Fig. 5Dg, were able to represent the panicle's curving path well.

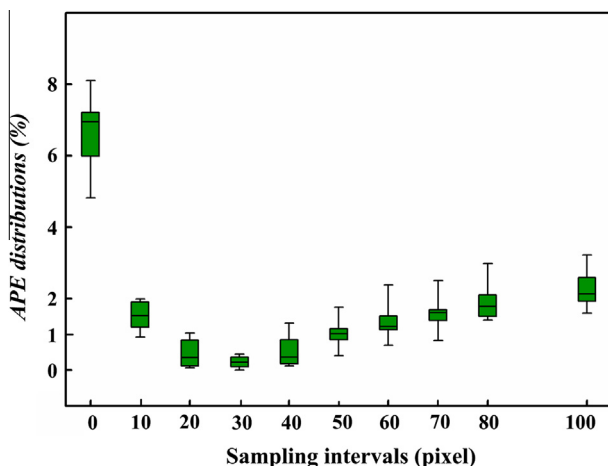


Fig. 6. Whole image analysis evaluation: APE distribution for different resampling intervals.

### 3.2. Neck identification accuracy

To evaluate the accuracy of neck identification, 100 randomly-selected panicle samples were utilized to identify neck position by both image analysis and human eyes. And the ordinates of neck position in the neck image (red line, as shown in Fig. 5Db) were recorded and compared. Automatic measurement was conducted with stem extraction, approximate neck region identification, neck segmentation and neck position computation. Meanwhile the manual measurement was performed by three skilled workers; they marked the neck ordinate in the neck image individually and the mean observation was taken as the ground truth.

The evaluation result of neck identification was shown in Table 2, and the absolute error distribution was exhibited in Fig. 7. From the results, the maximum error was 20 pixels, most of errors were less than 10 pixels, and the RMSE for neck identification was about 7.3 pixels, which meant 0.89 mm. therefore the results demonstrated that this neck identification method was reliable and the system could recognize the panicle neck with high accuracy.

### 3.3. System measuring accuracy

Panicles samples of Zhonghua 11 and Huageng 295, which had big morphologic difference, were used. Besides, both fresh samples and sun-dried samples, which had obvious color difference, were tested. Therefore, four batches of rice panicles including 100 fresh panicles from Huageng 295, 100 sun-dried panicles from Huageng 295, 100 fresh panicles from Zhonghua 11, and 100 sun-dried panicles from Zhonghua 11, were measured to evaluate the system's measuring accuracy. And PL results measured by the system and manual method (as previously mentioned) were compared.

The evaluation results of the system measurement for the above panicle samples was shown in Table 2. And the results shown that MAPE and RMSE results were respectively 0.92% and 2.24 mm for the fresh panicles from Huageng 295, 0.96% and 3.22 mm for the fresh panicles from Zhonghua 11, 1.34% and 3.20 mm for the sun-dried panicles from Huageng 295, and 1.69% and 5.14 mm for the sun-dried panicles from Zhonghua 11.

The results proved that automatic measurements had an excellent agreement with manual measurements and it was concluded that the *Smart-PL* system generally performed with high accuracy, an average MAPE of 1.23%. From the results, the measuring accuracy for the sun-dried panicles was with a little decrease, because the sun-dried panicle samples had a relatively low contrast between stem and neck, and it would decrease the precision for neck identification. Meanwhile the results also shown that the measuring accuracy for Zhonghua 11 was lower than Huageng 295, because Zhonghua 11 (as shown in Fig. 1d) was bent more and had more complicated panicle type than Huageng 295 (as shown in Fig. 1b), which would increase the difficulty of image processing for path extraction. But the results also proved that the system had a good performance for these panicle types in general. Finally, the *Smart-PL* system demonstrated to be a high-precision way to measure panicle length, regardless of the panicle type.

### 3.4. System stability and measuring efficiency

To evaluate the system's efficiency, 3108 randomly selected panicle samples were tested under continuous-measurement conditions, and the measurement result was shown in Table 2. The MAPE and RMSE for the measurements was 1.86% and 6.43 respectively. The results demonstrated that the *Smart-PL* system had a good performance in stability and reliability.

The *Smart-PL* system worked including 5 steps as described in Section 2.3 and measurement time for each panicle was calculated by Eq. (1). Accordingly, the manual measurement for each panicle

**Table 2**  
The results of the system evaluation.

Measurement	Panicle samples	Panicle number	$R^2$	MAPE (%)	RMSE (mm)
Whole image analysis evaluation	Panicles with neck cut off	100	0.99	0.39	1.19
Neck identification evaluation	Randomly-selected	100	0.99		0.89
System measurement evaluation	Fresh Huageng 295	100	0.97	0.92	2.24
	Sun-dried Huageng 295	100	0.95	0.96	3.22
	Fresh Zhonghua 11	100	0.98	1.34	3.20
	Sun-dried Zhonghua 11	100	0.96	1.69	5.14
Continuous measurement evaluation	Randomly-selected	3108	0.98	1.86	6.43

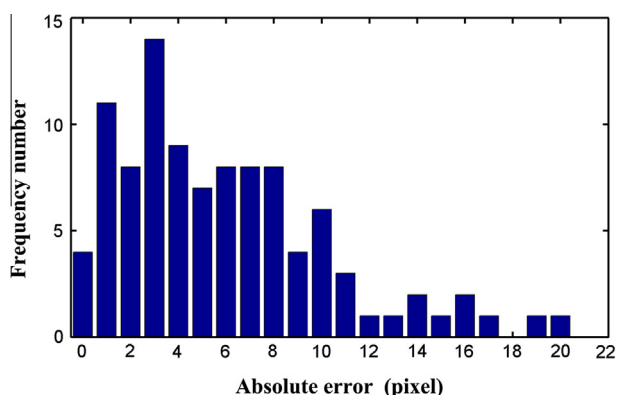


**Fig. 7.** The absolute error distribution for neck identification.

was performed with following procedure: identifying the neck of the rice panicle, straightening the panicle, measuring the panicle length, recording the result, and the measurement time for each panicle is the sum of time cost of the above procedures. All the measurement was performed continuously, meanwhile the time costs of manual measurement and automatic measurement were both recorded. It took approximately three and one-half hours to measure the 3108 panicle samples using the system; i.e., the system efficiency was approximately 900 panicles per hour. By contrast, it took nearly 3 working days for a skilled worker to complete the measurements manually. Thus, the system was almost 6 times as efficient as the manual method.

The experimental results indicated that it took about 4 s for the system to measure a panicle. Generally, it took approximately 1 s to place the panicle and 2 s to take it out and begin the next measurement. The panicle length was extracted in approximately 1 s on a workstation configured with a 2.3 GHz main frequency, 3 GB of memory, and 4 CPU cores. Image acquisition and result storage required less than 0.1 s. Therefore, the manual operation of the system (placing the panicle and taking the panicle out) was still time-consuming, which accounted for approximately three quarter of the measurement time of the system. Moreover, manual operation of the system was tedious in the continuous-measurement mode. To improve them, an automatic panicle transport platform might be incorporated in the practical promotion.

#### 4. Discussion

Rice panicle length is one of the most important yield-related traits, defined as the length from the panicle neck to the apex (Xiao et al., 1998). However the traditional method for panicle length measurement is still manual, which is subjective and slow. And there were few efforts to develop the automatic panicle length measuring technique. LemnaTec Corporation developed a Plant Phenotyping system, which can estimate rice panicle length in vivo, but the neck cannot be recognized. To achieve it, dual cam-

era imaging were demonstrated, and the high-resolution image were provided for neck identification. Meanwhile the specific algorithms for neck identification were proposed, and the results proved that it had a good performance. Ikeda developed software to extract panicle length from scanned photographic images of spread-out panicles (Ikeda et al., 2010), however few details about the software were revealed and the image acquisition was time-consuming. To improve it, charge-coupled device (CCD) camera was adopted, and specific algorithms for panicle length extraction were developed. Moreover the whole processes of image acquisition, image analysis, and data storage are integrated and performed automatically. The results demonstrated that the measuring efficiency was approximately 900 panicles per hour. Therefore this study demonstrated a novel prototype for high-throughput, high-precision and low-cost measurement of rice panicle length, which was able to be applied in the practical measurement.

#### 5. Conclusion

This paper describes a new prototype, called “Smart-PL” for the efficient and automatic measurement of rice panicle length. Dual-camera imaging was employed to provide a neck image for neck identification and a whole-panicle image for path extraction. Equipped with dedicated software for system control and image analysis, the *Smart-PL* system was able to identify panicle neck accurately and finally extract panicle length with high accuracy, regardless of panicle type. Therefore this system could be applied in rice breeding for panicle trait evaluation, providing reliability and high efficiency. The system is a new application of agricultural photonics, the objective of which is to improve breeding by using various imaging technologies (Finkel, 2009). In conclusion, the *Smart-PL* system provides a novel tool for rice yield-related research.

#### Acknowledgements

The authors deeply appreciate their partners at Huazhong Agricultural University for providing panicle samples. This work was supported by the National High Technology Research and Development Program of China (863 Program, Grant No. 2010AA10Z203), the Key Program of the Natural Science Foundation of Hubei Province (Grant No. 2008CDA087), and the Program for New Century Excellent Talents in the University (No. NCET-10-0386).

#### References

- Bagge, M., Lubberstedt, T., 2008. Functional markers in wheat: technical and economic aspects. *Molecular Breeding* 22 (3), 319–328.
- Chao, K., Chen, Y., Hruschka, W., Gwozdz, F., 2002. On-line inspection of poultry carcasses by a dual-camera system. *Journal of Food Engineering* 51, 185–192.
- Cheng, F., Zhang, Q., Zhu, H., Zhao, N., Wang, F., Chen, K., Zhang, G., 2007. The difference in amylose content within a panicle as affected by the panicle morphology of rice cultivars. *Journal of Cereal Science* 46, 49–57.

- Duan, L., Yang, W., Bi, K., Chen, S., Luo, Q., Liu, Q., 2011. Fast discrimination and counting of filled/unfilled rice spikelets based on bi-modal imaging. *Computers and Electronics in Agriculture* 75, 196–203.
- Finkel, E., 2009. IMAGING With 'Phenomics', plant scientists hope to shift breeding into overdrive. *Science* 325, 380–381.
- Ikeda, M., Hirose, Y., Takashi, T., Shibata, Y., Yamamura, T., Komura, T., Doi, K., Ashikari, M., Matsuoka, M., Kitano, H., 2010. Analysis of rice panicle traits and detection of QTLs using an image analyzing method. *Breeding Science* 60, 55–64.
- Joen, J.S., Jung, K.H., Kim, H.B., Suh, J.P., Khush, G.S., 2011. Genetic and molecular insights into the enhancement of rice yield potential. *Journal of Plant Biology* 54, 1–9.
- Jung, J.H., Choi, Y., Hong, K.J., Min, B.J., Choi, J.Y., Choe, Y.S., Lee, K.H., Kim, B.T., 2009. Development of a dual modality imaging system: a combined gamma camera and optical imager. *Physics in Medicine and Biology* 54 (14), 4547–4559.
- Kaizu, Y., Imou, K., 2008. A dual-spectral camera system for paddy rice seedling row detection. *Computers and Electronics in Agriculture* 63 (1), 49–56.
- Kato, Y., Nemoto, K., Yamagishi, J., 2009. QTL analysis of panicle morphology response to irrigation regime in aerobic rice culture. *Field Crops Research* 114, 295–303.
- Kobayashi, K., Horie, Y., Imaki, T., 2002. Relationship between apical dome diameter at panicle initiation and the size of panicle components in rice grown under different nitrogen conditions during the Vegetative Stage. *Plant Production Science* 5 (1), 3–7.
- Liu, G., Mei, H., Liu, H., Yu, X., Zou, G., Luo, L., 2010. Sensitivities of rice grain yield and other panicle characters to late-stage drought stress revealed by phenotypic correlation and QTL analysis. *Molecular Breeding* 25, 603–613.
- Nemeth, G., Palagyi, K., 2011. Topology preserving parallel thinning algorithms. *International Journal of Imaging Systems and Technology* 21, 37–44.
- Otsu, N., 1979. A threshold selection method from gray-level histograms. *IEEE Transactions SMC* 8, 62–66.
- Wyant, J.C., Schmit, J., 1998. Large field of view, high spatial resolution, surface measurements. *International Journal of Machine Tools & Manufacture* 38, 691–698.
- Xiao, J., Li, J., Grandillo, S., Ahn, S., Yuan, L., Tanksley, S., McCouch, S., 1998. Identification of trait-improving quantitative trait loci alleles from a wild rice relative, *Oryza rufipogon*. *Genetics* 150, 899–909.
- Xing, Y., Zhang, Q., 2010. Genetic and molecular bases of rice yield. *Annual Review of Plant Biology* 61, 11.1–11.22.
- Yang, W., Xu, X., Duan, L., Luo, Q., Chen, S., Zeng, S., Liu, Q., 2011. High-throughput measurement of rice tillers using a conveyor equipped with x-ray computed tomography. *Review of Scientific Instruments* 82, 025102-1–025102-7.
- Yang, X., Gong, H., Quan, G., Deng, Y., Luo, Q., 2010. Combined system of fluorescence diffuse optical tomography and microcomputed tomography for small animal imaging. *Review of Scientific Instruments* 81, 054304-1–054304-8.
- Zhu, J., Zhou, Y., Liu, Y., Wang, Z., Tang, Z., Yi, C., Tang, S., Gu, M., Liang, G., 2011. Fine mapping of a major QTL controlling panicle number in rice. *Molecular Breeding* 27, 171–180.